Journal of Computer Science

Research Article

Transfer Learning-Driven Binary Classification of Chest X-ray for Pneumonia Using Deep Convolutional Architectures

Nusrath Fathima and Pradeep Kumar

Department of CS and IT, Maulana Azad National Urdu University, Hyderabad, Telangana, India

Article history
Received: 15-07-2025
Revised: 05-12-2025
Accepted: 08-12-2025

Corresponding Author:
Nusrath Fathima
Department of CS and IT, Maulana Azad National Urdu University, Hyderabad, Telangana, India
Email: nusrath.fathima@manuu.edu.in

Abstract: Pneumonia is the most common infectious cause of lung inflammation, resulting from the presence of viruses or bacteria in the microscopic air sacs. In recent years, artificial intelligence, particularly deep learning, has gained significant traction in the field of medical imaging. Early detection and diagnosis of pneumonia using chest X-rays can support radiologists in clinical decision-making and subsequent treatment planning, thereby helping to reduce mortality rates. In this study, a chest X-ray dataset was used to classify images for pneumonia detection using transfer learning with four deep learning architectures: Visual Geometry Group 16 (VGG16), DenseNet201, Inception V3, and Inception ResNet V2. Each model was developed, implemented, and evaluated, and the results were analyzed and compared. The best-performing model was identified based on accuracy and minimal loss, demonstrating promising proficiency and robustness. The dataset employed in this study was obtained from Kaggle. The methodology involved data collection, preparation, preprocessing, and visualization. Models were developed and implemented using the Jupyter Notebook editor via Google Colaboratory. Among the architectures evaluated, DenseNet201 achieved superior performance compared to VGG16, Inception V3, and Inception ResNet V2 in terms of classification accuracy.

Keywords: Pneumonia Detection, Deep Learning Architectures, Transfer Learning, Chest X-Ray

Introduction

Pneumonia, a severe infectious inflammatory condition in the air sacs of one or both lungs, is a significant health concern worldwide (Elgendy, 2020). The presence of bacteria, fungi, or viruses leads to symptoms of cough, fever, and breathing difficulties. Chest X-rays play a pivotal role in the diagnosis of pneumonia identification as they provide a clear visual representation of the lungs that aid physicians in detecting abnormalities that lead to the indication of the presence of infection. Diagnosing pneumonia using chest X-rays entails evaluating lung opacities, which show up as lighter areas on the X-ray image (Johnson and Wells, 2019). These opacities indicate spots where air spaces are occupied by fluid, pus, or other cellular material instead of air (Asswin et al., 2023). This condition can present in different forms, such as lobar pneumonia, affecting a single lobe of the lung, or bronchopneumonia, which displays a more scattered, patchy pattern throughout the lungs (University of Utah Health, 2024).

The precision of pneumonia diagnosis via chest X-rays is significantly influenced by the proficiency of radiologists, who are tasked with differentiating pneumonia from other medical conditions that exhibit similar radiographic characteristics, including congestive heart failure, lung cancer, and pulmonary edema (Baltruschat et al., 2019; Hammoudi et al., 2021). The dataset used contains images of healthy and pneumonia-infected individuals, as shown in Fig. 1. This interpretative task is inherently subjective, and the presence of qualified radiologists is frequently constrained, especially in resource-limited environments.

Among the different diagnostic tests (CT scan, lung ultrasound, lung x-rays, lung MRI) for pneumonia identification, Chest x-rays are considered one of the cost-effective and accessible diagnostic imaging techniques (Berliner et al., 2016; Sait et al., 2019).

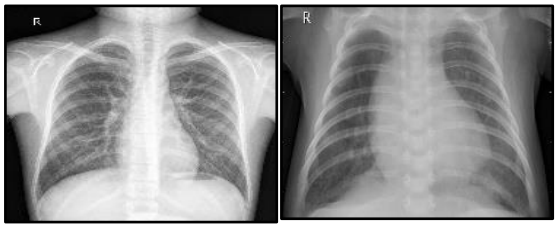

Fig. 1: (a) Normal x-ray (b) Pneumonia-infected x-ray

X-rays are favoured over CT scans due to the latter's extended duration and the restricted availability of high-quality CT scanners in several remote regions. X-rays represent the most frequent and accessible form of diagnostic process, performing a critical role in medical and epidemiological procedures (Sirish Kaushik et al., 2020). Numerous areas worldwide experience a shortage of trained healthcare professionals and radiologists, whose expertise is critical for accurate disease assessment (Al Mamlook et al., 2020; Swetha et al., 2021). The utilization of CAD through AI solutions is gaining traction, as it can be made accessible to a broad population at a minimal cost (Gabruseva et al., 2020; Attallah, 2021). A further complication in diagnosing pneumonia arises from the overlap of its symptoms with those of other diseases, which can pose challenges for radiologists (Sitaula and Hossain, 2021). Deep learning techniques address these issues, demonstrating predictive accuracy comparable to, and in some cases exceeding, that of an average radiologist (Hesamian et al., 2019). Among these techniques, neural networks have exhibited significant potential in image segmentation and classification, leading to their widespread adoption within the research community (Stephen et al., 2019). The application of deep learning and computer vision techniques in biomedical image diagnosis has proven beneficial in delivering rapid and accurate disease diagnoses that align with the reliability of experienced radiologists (Bhattarai and Od, 2023). However, it is essential to recognize that deep learning-based methodologies are not meant to replace trained medical professionals in the diagnostic process; instead, they are intended to augment the clinical decision-making framework.

Advancements in artificial intelligence and deep learning offer promising solutions to these challenges. Large chest x-ray image datasets, once trained, can learn to recognize the subtle differences and patterns associated with pneumonia (Elgendy et al., 2022). Transfer learning, which involves fine-tuning pre-trained models like InceptionV3, VGG16, DenseNet201, and Inception ResNetV2, has shown significant potential in enhancing the performance of these models, even with relatively small medical datasets (Shu, 2019). The implementation of advanced neural networks to automate the diagnostic process has the potential to substantially decrease the time required for diagnosis while enhancing accuracy (Pan and Yang, 2010). This approach offers dependable and consistent evaluations that can assist radiologists in making informed clinical decisions. The incorporation of deep learning techniques into medical imaging signifies a notable advancement in utilizing technology to tackle global health issues, especially in the enhancement of pneumonia detection and treatment (Al-kuraishy et al., 2020). This study employs a publicly accessible chest X-ray dataset for the purposes of training and validation, thereby ensuring the model's relevance to practical applications.

Though the individual deep learning architectures VGG16 (Sharma and Guleria, 2023), DenseNet (Sanghvi et al., 2023), Inception V3, and Inception ResNet (Brital, 2021) are explored as single models or an ensemble model for pneumonia detection, a direct systematic head-to-head comparison under a consistent transfer learning environment and controlled conditions is lacking. The rationale for choosing the said models is: VGG16 for the simplicity and depth of the model with baseline of 3x3 convolutions; DenseNet 201 for its parameter efficient design and robust dense connection aiding the vanishing gradient resolution; Inception V3 for the computational efficiency and ability of multi-scale varied feature extraction; and finally, Inception ResNet V2, hybrid model combining the advantages of Inception and ResNet models. This study aims to fill the gap by conducting a comprehensive comparative analysis that provides empirical evidence in the selection of an optimal model from architecturally distinct deep learning models. The novelty of this paper lies in the comparison of the top-rated four distinct deep learning models, each with its own strength, on the same Chest X-ray dataset with the same pre-processing techniques and hyperparameters for thorough analysis for real-world assessment. The results of this investigation could facilitate the wider implementation of automated diagnostic instruments in clinical settings, utilizing artificial intelligence to assist radiologists and optimize healthcare delivery.

The contributions made in this paper are

1. A robust deep CNN model is developed utilizing state-of-the-art deep learning architectures for the classification of the chest x-ray images as either healthy or infected with pneumonia
2. Four popular deep learning architectures – VGG16, DenseNet 201, Inception V3, and Inception ResNet V2 are trained by deploying a transfer learning approach on the Chest X-ray dataset

3. Feature extraction is performed using pre-trained deep learning architectures with a customized top layer to classify the input image as either Normal or pneumonia-infected, eliminating the necessity of manual feature extraction and reducing the load of radiologists in pneumonia detection
4. Data Augmentation is employed to mitigate overfitting, expand the dataset, and enhance the model's performance in diagnosing pneumonia cases
5. We evaluated the behavior and performance of the proposed models with the help of performance metrics – accuracy curves, loss curves, confusion matrix, and predictions summary
6. The results reveal that the proposed deep transfer learning architectures have performed better in terms of accuracy compared to the existing published work

Related Work

An ensemble model of four different pre-trained models was proposed for pneumonia presence by combining the outputs of all the models in the detection of pneumonia, utilizing the transfer learning approach by Chouhan et al. (2020). An amalgamation of EfficientB0 and DenseNet 121 architectures was proposed by An et al. (2024), using the attention mechanism in the detection of pneumonia, and achieved an accuracy of 95%. Rahman et al. (2020) have reported three types of classifying pneumonia with the transfer learning approach on the deep learning architecture – AlexNet, ResNet18, DenseNet 201, and SqueezeNet. Ibrahim et al. (2024) have created a deep learning model utilizing Alex Net architecture to facilitate the classification of COVID and pneumonia through analysis of X-ray scan images applicable for both binary and multi-class classification.

An advanced fine-tuned VGG16 architecture was introduced by Chhabra and Kumar (2022) for detecting pneumonia, engaging the strategies of transfer learning on the chest X-ray images, and attained an accuracy of 93.6%. To detect and classify pneumonia, Gabruseva et al. (2020) employed the single-shot detectors for region detection, squeeze and extinction CNNs, augmentation, and multi-task learning computational approaches. Liang and Zheng (2020) have applied a residual architecture with diluted convolution using transfer learning algorithms for the automated classification of paediatric pneumonia and achieved an accuracy of 96%. El Asnaoui et al. (2021) performed a comparison of fine-tuned versions of different deep learning architectures for automatic pneumonia detection using the chest X-rays and CT scan images and concluded that Resnet50 has shown highly satisfactory results among all architectures used, with the main limitation being the unbalanced dataset. Phine (2023) developed a deep learning model for pneumonia detection and classification using the VGG19 architecture and achieved an accuracy of 86 and 94% for the unbalanced and balanced chest x-ray datasets, respectively. Siddiqi and Javaid (2024) have conducted an extensive, comprehensive analysis of Deep learning applications in the detection of pneumonia using chest x-ray and addressed the effective results of the Vision transformers technique and its limitations, along with the fundamental research scope that can be carried out.

Patil et al. (2024) implemented a deep learning model using VGG16 and ResNet50 architectures and achieved a maximum accuracy of 87.5% using the ResNet50 model. Jain et al. (2022) have used Xception, VGG16, and VGG19 deep learning models to predict COVID-19-induced / regular pneumonia using the transfer learning approach. Szepesi and Szilágyi (2022) have suggested a CNN model focusing on the dropout layer placement in the architecture that has yielded a good accuracy of 97% in pneumonia detection. Lamia and Fawaz (2022) have presented a mobile pneumonia detecting application with the aid of neural networks and achieved an accuracy between ~78 to ~85%.

Unlike the traditional machine learning approach, deep learning approaches are not dependent on domain expertise and hand-crafted features. The features are automatically being learned using back propagation techniques (Le Cun et al., 2015). The high-quality chest x-ray datasets that are publicly available have enhanced the research studies, and recently, using the Generative Adversarial Networks (GANs), synthetic chest x-ray techniques (Srivastav et al., 2021) are employed to overcome the generalization and the overfitting issues. Motamed et al. (2021); Sharma and Guleria (2023) have investigated the VGG16 deep learning architecture with different classification algorithms Support Vector Machine, Random Forest, Naïve Bayes, Neural Networks, and K-Nearest Neighbour using two distinct chest x-ray image datasets and concluded that VGG16 with Neural Networks has exhibited a promising accuracy in comparison to other classification algorithms. Jiang et al. (2021) developed an improved VGG16 model IVGG13 model with reduced layers, performed a comparison with LeNet, AlexNet, GoogLeNet, and VGG16 for the detection of pneumonia, and concluded the effectiveness of data augmentation on the model's accuracy. Since the COVID-19 pandemic outbreak, lung ultrasound imaging has gained popularity as a quick, adaptable, and non-invasive diagnostic tool for lung diseases. Considering this, Ni et al. (2024) designed a Multi-Enhanced Views Active Learning model for precise classification of the lung ultrasound image patterns. Ouis and Akhloufi (2024) emphasized the use of deep learning in the advancement of radiology report production, considering the chest x-ray image analysis and the need for better patient care, less workload on radiologists by enhancing AI's role in radiology insights.

A new assessment technique was proposed by Jeong et al. (2022) as the OVASO model based on the integrated binary CNN model that selectively chooses a 1 vs-all and 1-vs-1 classifier for the classification of chest x-rays. Sanghvi et al. (2023) developed a web application to classify the radiographs of chest x-rays as COVID and pneumonia using the DenseNet 201 deep transfer learning approach. Four hybrid models from the combination of pre-trained deep learning architectures VGG19 (V), Inception (I), Dense Net (D), and Mobile Net (M) were proposed by Gupta et al. (2023) for the multi-class classification of chest x-ray, in which the model VMD has outperformed when implemented using five-fold cross-validation. Mathivanan et al. (2024) have utilized transfer learning for four deep learning architectures to classify the brain tumours using MRI scans. El-Latif et al. (2024) proposed an automated ovarian cancer prediction deep learning model based on fuzzy logic and achieved an accuracy of 98.99%. Mavaddati (2024) investigated a 50-layer ResNet architecture for brain tumor classification using deep transfer learning.

Jain et al. (2024) proposed a multi-class classification of lung tumour using deep reinforcement transfer learning and achieved a remarkable accuracy of 99.40%. Trivedi and Gupta (2022) proposed a deep learning model based on MobileNet architecture and achieved an accuracy of 97.3% and 87.3% for training and testing phases, respectively. Colin and Surantha (2025) have evaluated the four interpretability techniques Layer-wise Relevance Propagation (LRP), Adversarial training, Class Activation maps, and Spatial Attention Mechanism for the deep learning architectures – ResNet 50, and concluded that LRP is most effective in maintaining the accuracy. Sarvari and Sridevi (2025) have presented a reliable and efficient hybrid deep learning model based on CT scan images for COVID-19 detection that outperformed the traditional algorithm results. Xu et al. (2022) performed extensive evaluations on deep learning models for chest x-ray images in edge computing for the detection of coronavirus. Chakraborty et al. (2025) proposed a lightweight and computationally efficient DeepPneuNet model for the prediction of pneumonia and achieved 90.12% accuracy. Mohamed Abueed et al. (2025) performed a systematic, extensive literature review on transfer learning in combination with other methods for pneumonia detection and categorized the models into deep learning, transfer learning, and hybrid on the basis of research papers from reputed research repositories like ACM, Elsevier, IEEE, Springer, etc., and concluded with the potential of the transfer learning techniques in pneumonia detection and clinical applications optimization on a broader scale.

Materials and Methods

In this study, the different deep learning architectures VGG16, Dense Net 201, Inception V3, and Inception Res Net V2 are developed with the transfer learning strategy. Transfer learning refers to the learning of features and applying them to a new model from the knowledge gathered by training a different model architecture. The performance and training are accelerated by recycling the learned features, especially in data scarcity scenarios (Asif et al., 2023). The programming language used for this study is Python. Scikit learn libraries, matplotlib, OpenCV, and Keras applications are used for model development and visualizations. The flow diagram of the carried-out experiment is shown in Fig. 2.

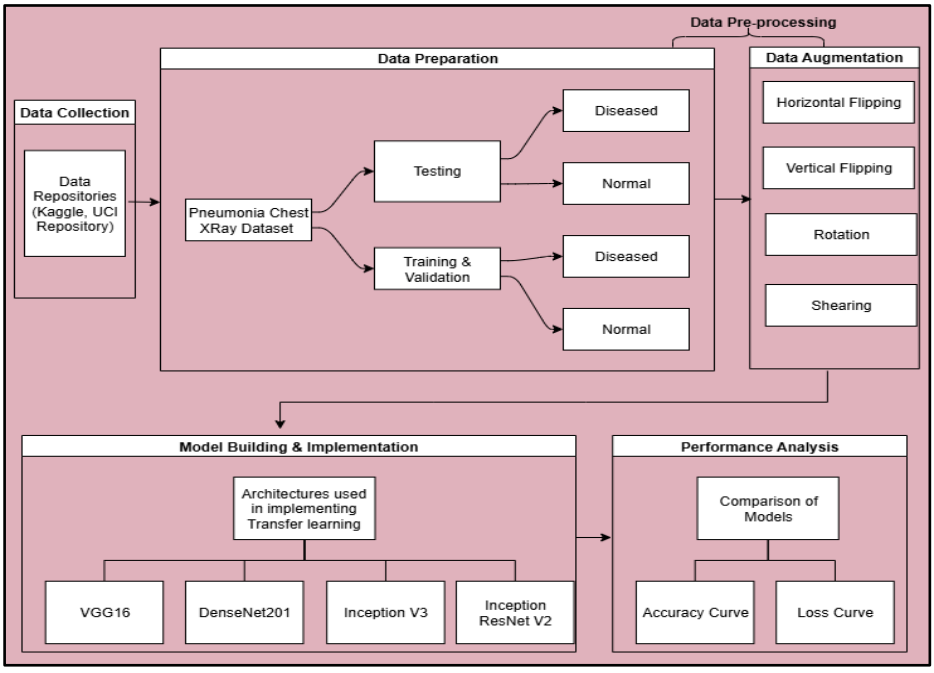

Fig. 2: Flow diagram of the proposed work

The experiment starts with the Data collection phase, followed by the Data preparation and pre-processing phase. The dataset is collected from the publicly available repositories. While the standard dataset repositories are crucial for research, they may have constraints with regard to inherent biases, image quality due to patient positioning, contrast, or exposure, and the instrument used for collection. To mitigate this, enriching the dataset with diverse clinical images can enhance the robustness and real-time deployment of the model. After pre-processing, to avoid overfitting, data augmentation is carried out to improve the diagnosis. The models are developed and implemented using Google Collaboratory. The performance of the models is studied in the analysis phase. The detailed description of each phase is explained in the following sub-sections.

Data Collection and Preprocessing

The Chest X-ray dataset contains a total of 6084 images that were collected from Kaggle for experimentation. The Chest X-ray dataset is binary classified as Normal (3019) and Diseased (3065). To avoid data imbalance in this study, the images are partitioned with almost the same number for both classes, as shown in Fig. 3(a). For the effective training and evaluation of performance, the standard proportion of train and test split is carried out on the dataset as 80:20, as shown in Fig. 3(b). A validation split of 0.2 is done on the training sample to evaluate the validation performance. Testing of the model performance is done on an unknown sample of 0.2 of the complete datasets.

Data Augmentation

The data augmentation technique is used for data generalization and the generation of more training data to avoid overfitting during the training process. The main aim is that the model will not visualize the same data twice and will be capable of adapting to real-world scenarios. This operation is carried out by using Keras with the ImageDataGenerator method for the transformations consisting of rotation, flipping, and sharpening. The visual of data augmentation carried out is shown below in Fig. 4.

Deep Neural Network Layers

Deep learning has become an exceptionally powerful and effective means for research and development, primarily due to its proficiency in managing large amounts of data. The Convolution Neural Networks (CNNs) represent the most used architectures in the realm of deep learning. A significant advantage of CNNs lies in their ability to analyse image features without regard to their spatial position. The distinct layers in the CNN include the Convolution layer, the Pooling layer, the Activation layer, and the fully connected layer.

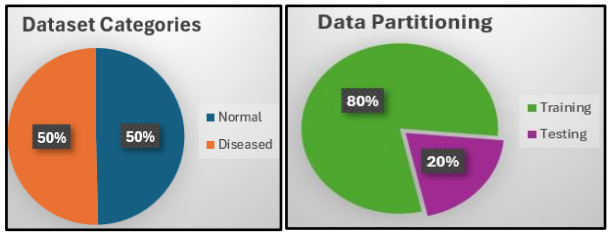

Fig. 3: (a) Distribution of Dataset categories (b) Data partitioning of the Chest X-ray dataset

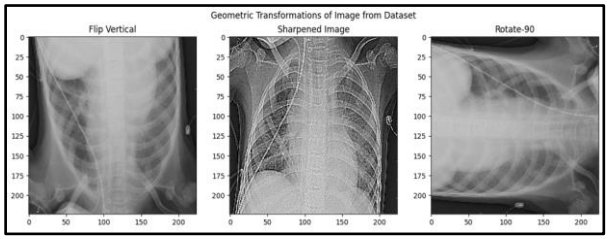

Fig. 4: Geometric Transformations of the image from the dataset

A convolution layer is the main building block that consists of a kernel or filters and learnable parameters to extract the significant features from the input. The shape of the input tensor is (inputs x height x width x channels). This, after going through the convolution, is mapped to a feature map with an activation function of shape (inputs x feature map height x feature map width x feature map channels). The different filters that can be applied to the convolution layer are [2x2], [3x3], [5x5], and [7x7]. As the filter changes, the regions of data that contribute to the significant attribute changes during the training process.

The operation carried out in the convolution layer using Eq. 1 is demonstrated below in Fig. 5(a) using an input feature map of size 6 x 6 and filter size 3 x 3:

$$h_{i,j} = \sum_{p=1}^{m} \sum_{q=1}^{m} w_{p,q} x_{i+p-1,j+q-1} \quad (1)$$

Pooling layers are the layers used in combination with the convolution layer that aid in reducing the dimensions of the data by combining the outputs of one layer into a single neuron in the next layer. The commonly used pooling size is 2x2. The two types of pooling that can be applied to a convolution layer can be local or global, and Max pooling or Average pooling. Local pooling involves small clusters of size 2x2. Global pooling works on the feature map, Max pooling uses the maximum value of the cluster map, and Average pooling considers the average value of the cluster. The pooling operation is demonstrated using the feature map in Fig. 5(b), and Eq. 2 is used for max pooling:

$$h_{i,j} = max\{x_{i+p-1,q+l-1} \; \forall \; 1 \leq p \leq m \; and \; 1 \leq q \leq m\} \quad (2)$$

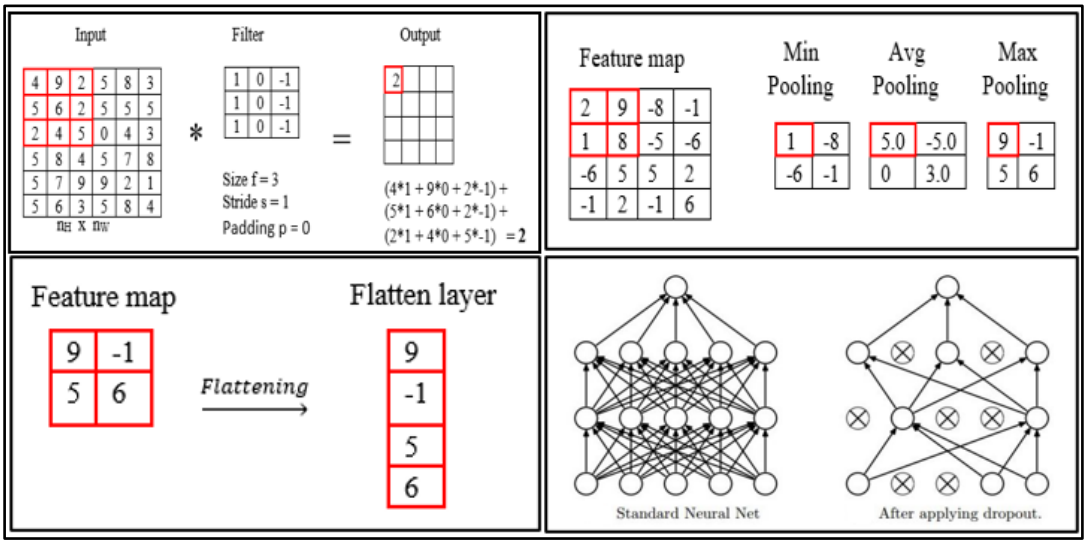

Fig. 5: (a) Convolution operation working, (b) Pooling operation working, (c) Flatten operation working, (d) Dropout representation

Activation layer refers to the activation function used to adjust and limit the negative values formed as the output of the convolution layer to reframe the network into a non-linear form to speed up the learning process. The different activation functions that can be used are ReLU, PReLU, tanh, sigmoid, etc. In our study, we have used the RELU activation function in the convolution layers, as the gradient is very small, making descent slow, as represented in Eq. 3. Sigmoid activation function for the binary classification in the output layer, as the $f(x)$ contains values between 0 and 1, as represented in Eq. 4:

$$g(z) = \max(0, z) \;\; ; \;\; g'(z) = \begin{cases} 0 & z < 0 \\ 1 & z \geq 0 \end{cases} \quad (3)$$

$$f(x) = \frac{1}{1 + e^{-(x)}} \quad (4)$$

A fully connected layer is a single-dimensional feature vector of the feature map that is obtained after all the convolution layers and the pooling layers. This fully connected layer is used to classify the different categories of images. The fully connected layer is represented as a single vector by converting the feature map into a single dimension, as shown below in Fig. 5(c). Dropout layer is one of the regularization and optimization techniques used during the training phase to prevent overfitting, and is always found after the dense layers, as these dense layers have more parameters than convolution layers. Therefore, the dropout layer must be carefully positioned while creating larger and more accurate models (Wager et al., 2013). The working of the dropout layer is shown below in Fig. 5(d).

Model Building Using Transfer Learning

Deep Neural Network models for Pneumonia detection/ classification of Chest x-ray and transfer learning: Deep neural network pre-trained models VGG16, DenseNet201, Inceptionv3, and Inception ResNetv2 are used for classification/prediction. These models have been proposed by many researchers as segmentation-free methods and are used as feature extractors (Sevli, 2022). Transfer learning is a technique that refers to making use of a model trained on a different large dataset and training only the fully connected layers for classification/prediction, thereby drastically reducing the computational complexity (Shin et al., 2016). The architectures and the performance of the models developed using transfer learning are summarized in the following paragraphs Fig. 6 illustrates the different approaches to solving a task. In the traditional approach, different tasks are trained, and learning models are developed specifically for each task. In contrast to the traditional approach, the transfer learning approach involves knowledge transfer from the source task training to the target task handling.

Figure 7 illustrates the different scenarios of transfer learning in a deep learning environment t(Elgendy, 2020). The fine-tuning of the layers of a deep learning model is described based on the size of the datase t (Elgendy, 2020).

The Scenario-1 way of transfer learning refers to freezing all the layers of the feature extraction of the pre-trained model and updating the final output layers.

In Scenario-2, the developer uses a pre-trained architecture of a similar dataset, freezes some layers, and utilizes some of the layers of the pre-trained architecture or appends custom layers for the feature extraction, modifies the dense layers, and the final output classification layer with the desired number of available classes in the dataset.

In Scenario 3, the small dataset that is different from the source dataset requires the developer to build custom layers for feature extraction and classification, utilizing very few layers from the pre-trained architecture. Scenario 4 demonstrates the training of the entire model in a custom way, where the user builds all the convolution layers, pooling layers, and dense layers from scratch based on any architecture, trains it on the dataset, and evaluates the model.

The different pre-trained deep neural network architectures used from the keras application for this study are shown in Table 1.

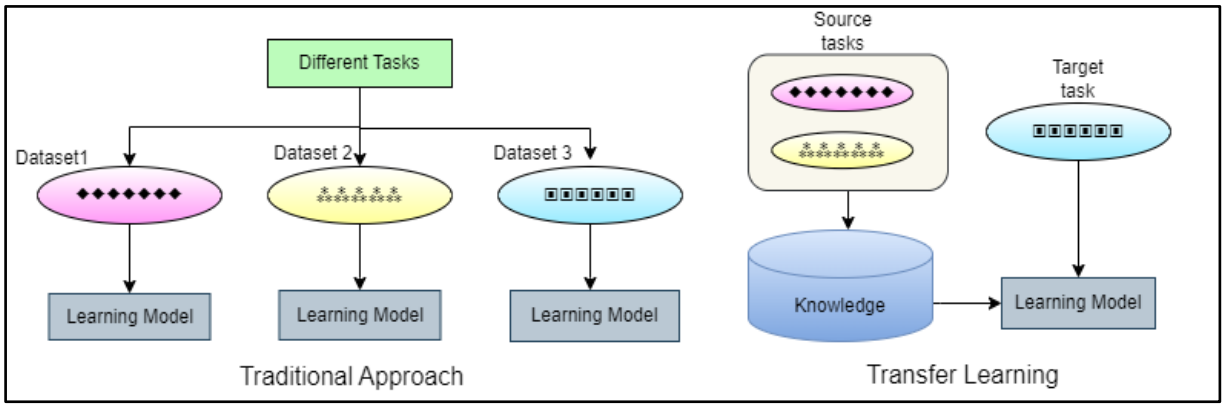

Fig. 6: Traditional Vs Transfer Learning approach

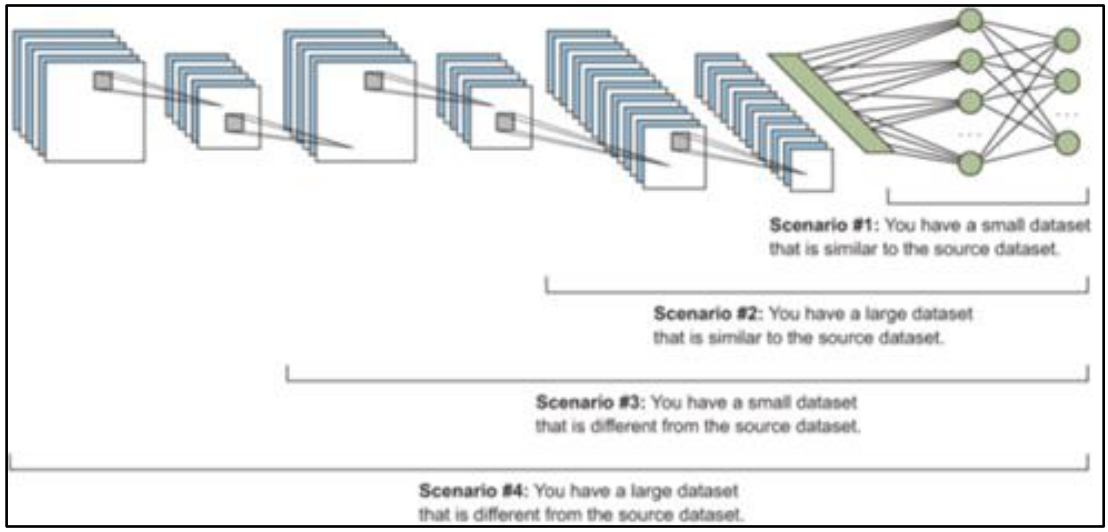

Fig. 7: Different scenarios of Transfer learning implementation in deep learning (Elgendy, 2020)

Table 1: Pre-trained architectures and their significant features

Network	Depth (Weight layers)	Size (in MB)	Parameters (millions)	Image input size
VGG16	16	515	138	224 x 224
Dense Net 201	201	77	20.0	224 x 224
Inception V3	48	89	23.9	224 x 224
Inception Res Net v2	164	209	55.9	224 x 224

VGG16 Architecture and Transfer Learning

VGG16 model supports 16 layers and is one of the top-5 test accuracy holders for the ImageNet dataset, having 1000 output classes (Boesch, 2021), . Large kernel size filters have been replaced by many 3x3 size filters, thereby surpassing the ground-breaking baseline object recognition tasks beyond the ImageNet dataset. The VGG16 model consists of five blocks with combinations of convolution layers and max pooling layers that are used for feature extraction. Using the transfer learning strategy, the top layer of the VGG16 architecture is modified, and

a customized top layer is appended for the classification and prediction corresponding to the classes of the dataset, as shown in Fig. 8.

From Figure 8, it is clear that the features are extracted using the standard VGG16 architecture by freezing the blocks and introducing the custom top layer with user-defined layers. The custom top layer consists of a pair of alternate Dropout and Dense layers with dropout values as (0.3, 0.2) and a dense layer with (relu activation function on 128 nodes, sigmoid activation function for 2 classes as outcomes), respectively. The layer summary of the proposed model is shown in Fig. 9.

DenseNet201 Architecture and Transfer Learning

Dense Net architecture is similar to Res Net architecture, with the exception of the feed-forward occurrence frequency updated to each layer to strengthen the information flow between the network layers. Dense Net 201 is 201 layers deep with direct connections, hence increasing information flow from one layer to the subsequent layers as feature maps (Jaiswal et al., 2021). The combined feature maps of current and previous layers demonstrate fewer parameters than the traditional CNNs.

The Dense block consists of three operations, namely the batch normalization, 3x3 convolution, and the ReLU activation function, while the transition layer is used after each dense block of three operations with 1x1 convolution and 2x2 max pooling to reduce the feature vector for the presence of any variations in the size of the previous output feature map.

After convolution and pooling operation on the input image, a sequence of dense blocks with three operations (Conv, BN, and Relu) and a transition layer with two operations(Conv, Pooling) is carried out four times with different numbers of iterations of operations in each layer (Mahum et al., 2023).

The fourth dense block and pooling layer are followed by the custom top layer to implement the transfer learning approach. The custom top layer with five different dense and dropout layers, followed by the classification layer, is appended to classify/predict with respect to the classes of the dataset. The architecture and the layered summary of the custom DenseNet 201 developed are shown in Fig. 10 and Fig. 11, respectively.

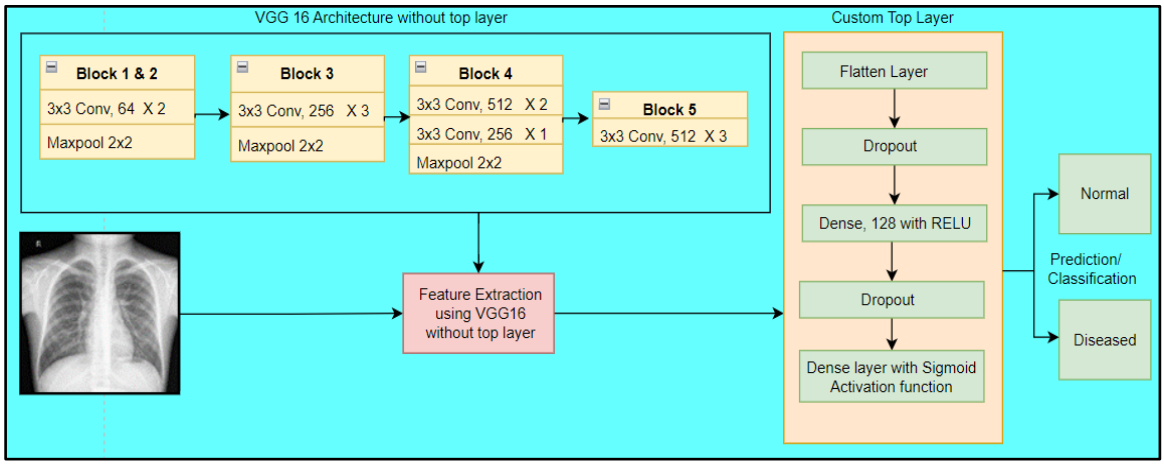

Fig. 8: Architecture of Customized VGG

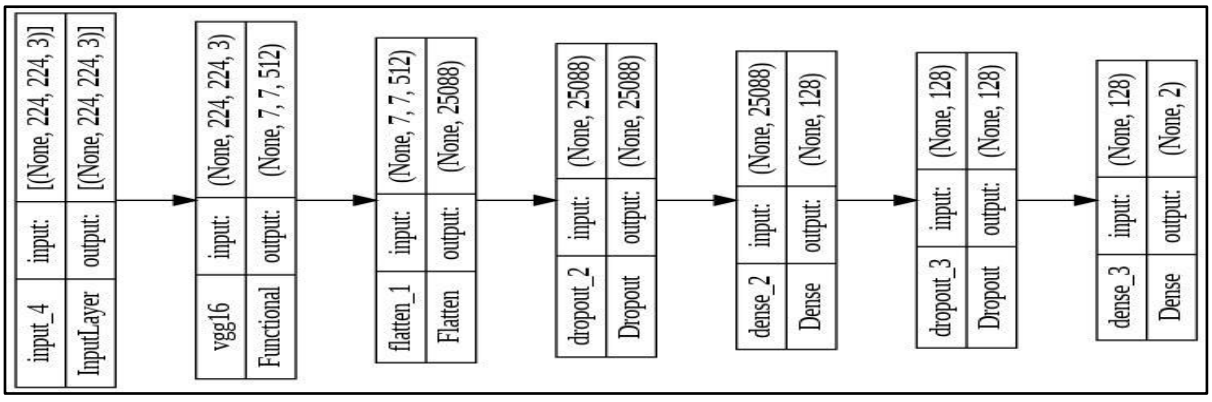

Fig. 9: Layer Summary of Customized VGG

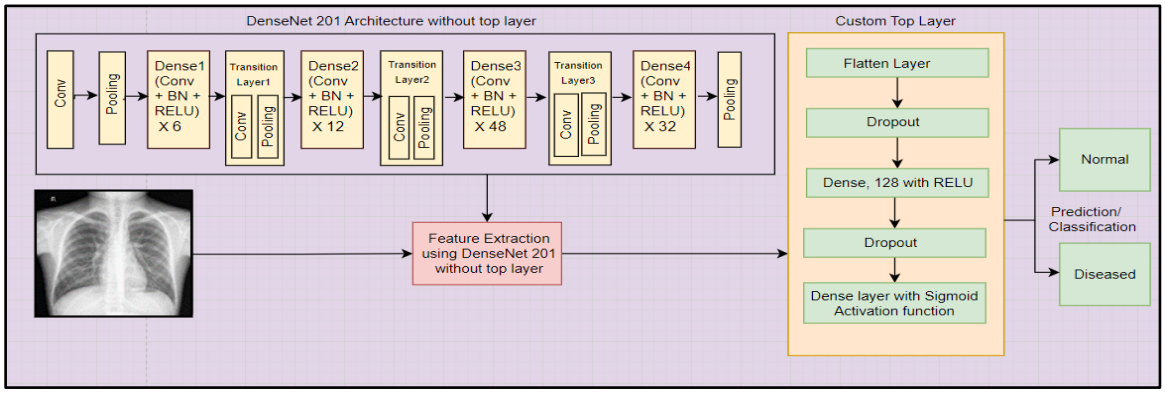

Fig. 10: Architecture of Customized DenseNet201 Architecture

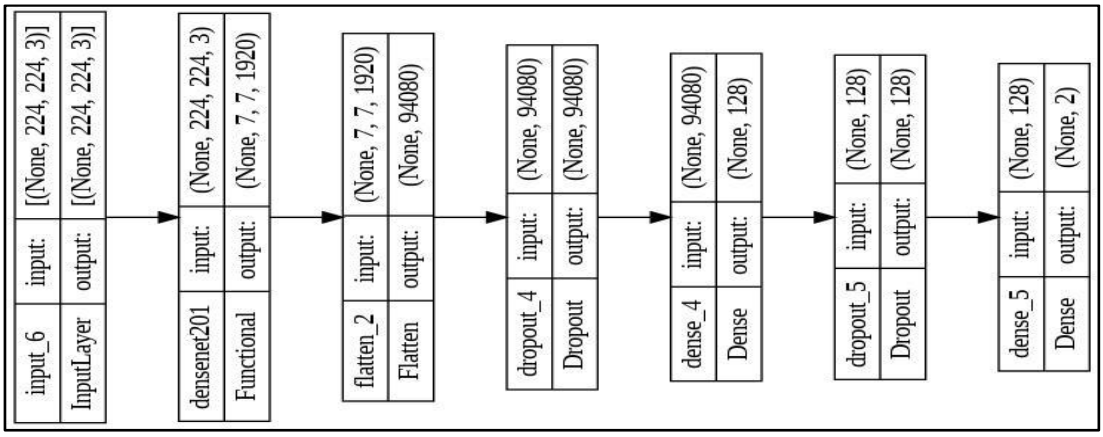

Fig. 11: Layer Summary of Custom DenseNet 201

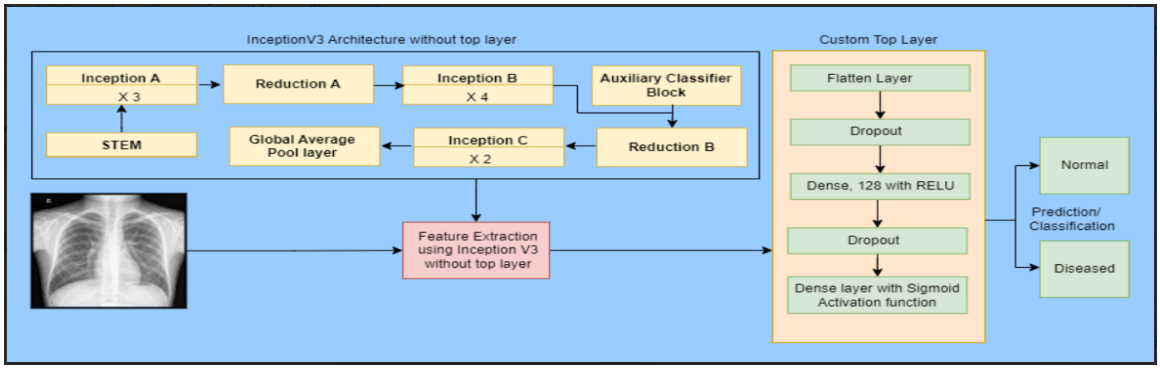

Fig. 12: Architecture of Customized InceptionV3 Architecture

InceptionV3 Architecture and Transfer Learning

Inception V3 is a powerful architecture, as the extraction of features is done at different scales using different kernels/filters. The top layer of the Inception v3 architecture is removed, and a custom top layer is introduced for the final classification/prediction of the image, depending on the dataset configuration. Inception V3 architecture has a depth of 48 layers, consisting of a normalization layer in addition to the convolution layers and pooling layers. The architecture starts with a stem block and a sequence of inception and reduction blocks, followed by the global average pooling layer and concluding with the softmax classifier along with logits (Brital, 2021). The custom architecture is developed by replacing the softmax classifier layer with a custom top layer having five layers of a series of dropout and dense, ending with a sigmoid binary classifier, as shown in Fig. 12.

Inception V3 architecture employs factorized convolutions, unlike large convolutions of different architectures, thereby reducing the computational speed and cost, leading to a major improvement in the extraction of features. The layer summary of the developed transfer learning model based on Inception V3 is depicted in Fig. 13.

Inception Res Net V2 Architecture and Transfer Learning

Inception Res Net V2 is a powerful architecture with combined advantages of Res Net and Inception architectures, incorporating residual connections with deeper network training, resulting in better extraction of features and preventing overfitting (Nguyen et al., 2018).

The top layer is replaced by the custom top layer with respect to the dataset utilized. Inception ResNet V2 architecture is a 169-layer deep network with a combination of Inception ResNet blocks and Reduction blocks with residual functionality aiding in solving the vanishing gradient problem. The transfer learning-based Inception ResNet v2 architecture implemented using a custom top layer is shown in Fig. 14.

The block diagram depicting the layers of the customized Inception ResNet V2 model is shown in Fig. 15.

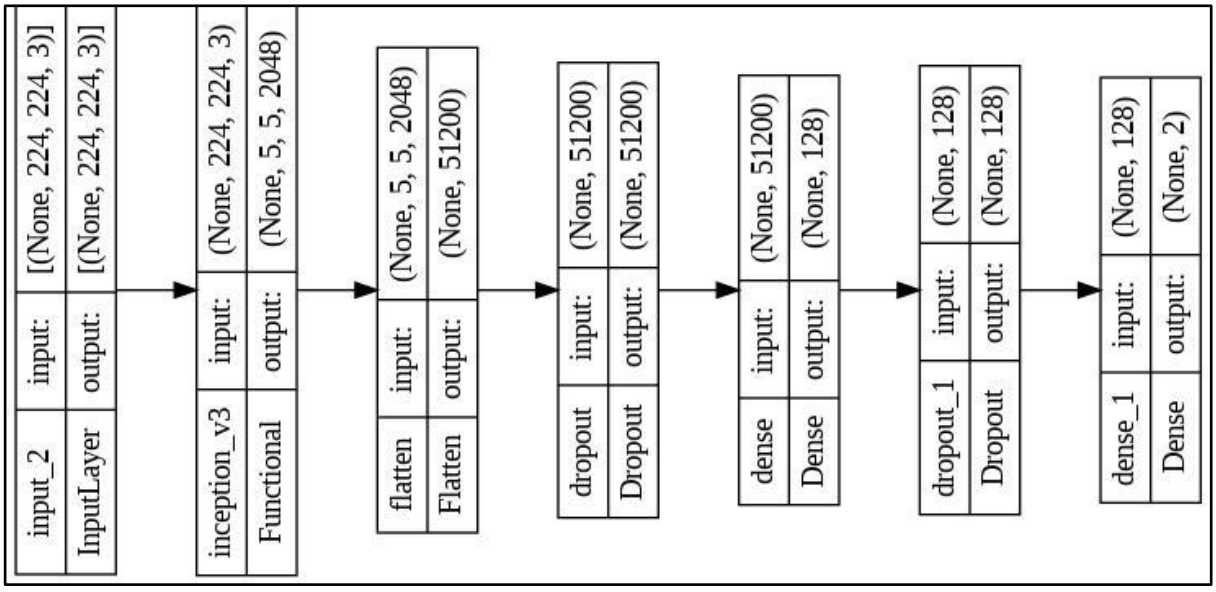

Fig. 13: Layer Summary of Custom Inception V3

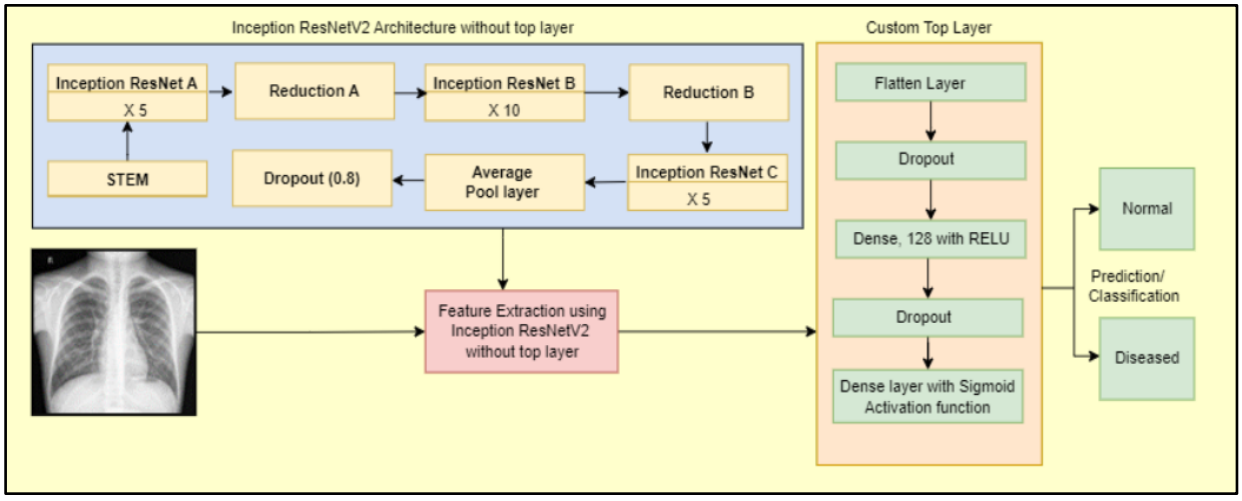

Fig. 14: Architecture of Customized Inception ResNetV2 Architecture

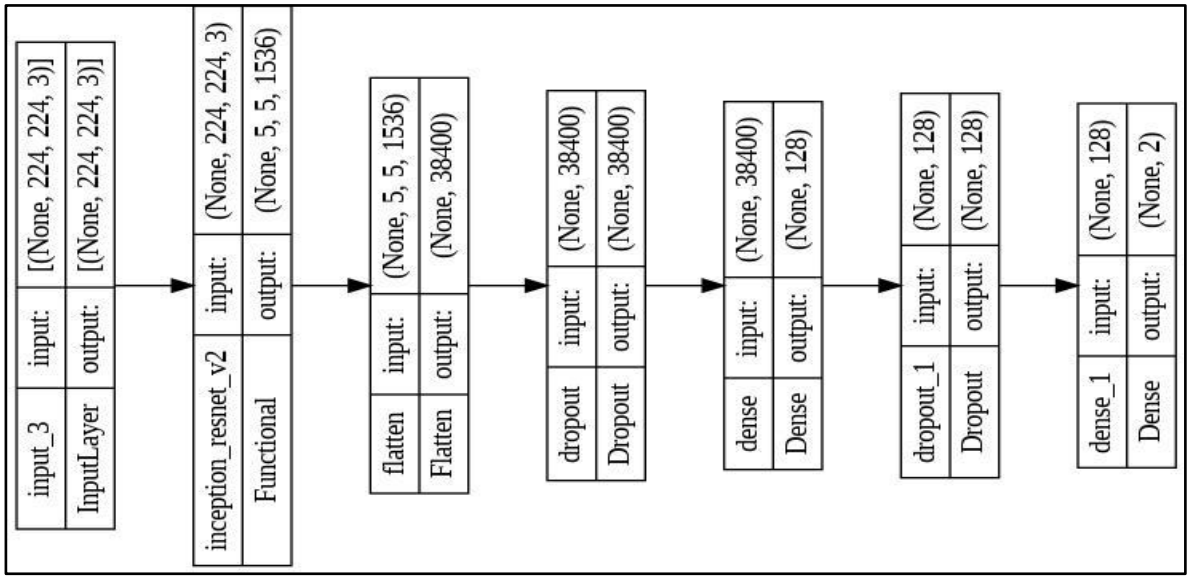

Fig. 15: Layer Summary of Custom Inception ResNetV2

The models VGG16, Dense Net 201, Inception v3, and Inception Res Net V2 were developed in Google Collaboratory using Jupyter Notebook in Python. Deep Learning models are built using TensorFlow and Keras applications. NumPy, sklearn, matplotlib, and seaborn libraries are used for calculations, data preprocessing, and data visualization. The models are partitioned into the feature extraction phase and the classification phase. In the feature extraction phase, the convolution layers and pooling layers are created considering the optimization methods by including the dropout layer, having mini-batches,, and including the learning rate decay with the Adam optimizer for better performance in terms of accuracy.

Results and Discussion

All the models, VGG16, Dense Net 201, Inception v3, and Inception Res Net V2, are executed for 25 epochs. As the epochs increased, the accuracy of the models has improved. The Adam optimizer with a learning rate of 0.0001 is used during compilation, and the loss function used is categorical cross-entropy. The validation accuracy of VGG16, Dense Net 201, Inception v3 and Inception Res Net V2 is 96.6, 97.1, 93.9 and 94.5% respectively in the training phase as shown in Fig. 16. The training phase of the models was accomplished over the learning iterations of 25 epochs with the size of the training dataset 4867 and out of 4867, the validation was done on 973 images for better understanding of the performance of the learning. The accuracy and the loss metrics determine the model's contribution to the dataset, its learning behavior, its robustness, and its generalization capability.

Fig. 16(a) represents the performance of the VGG transfer learning model in terms of accuracy, loss, and both curves in a clockwise direction in the respective block. The model is executed for 25 epochs. Initially, at epoch 1, the model reached an accuracy of 78%, and with each epoch, its learning improved. As it reached epoch 20, the learning appeared to be saturated and reached an acceptable level by epoch 25. The validation curve demonstrated excellent performance and robustness, and achieved 96%.

Dense Net 201 transfer learning model, on the other hand, started with 76% and progressively improved and reached a maximum 95% for the training sample and exhibited a maximum of 97% for an unseen training sample data, as shown in Fig. 16(b). The curves are the visualizations of the accuracy achieved for 25 epochs, the loss encountered for 25 epochs, and the plotting of accuracy and loss across the progression of the learning iterations in a corresponding block.

Beginning with 77% at epoch 0 to reaching 90% by epoch 25 for the training sample and for the validation sample, showing an upward trend by starting with 85% and culminating with 94% by epoch 25, the Inception v3 model has exhibited significant improvement in accuracy and a coherent decrease in the loss curve from 0.2 to 0.17 as shown in Fig. 16(c).

Fig. 16(d) illustrates the accuracy, learning curve, and the accuracy-loss curve of the Inception Res Net V2 model in a circular manner of respective block, demonstrating the divergence of training and validation accuracies over the epochs, and a coherent reduction in the loss is evidence of the model's proficiency in generalization of features learned.

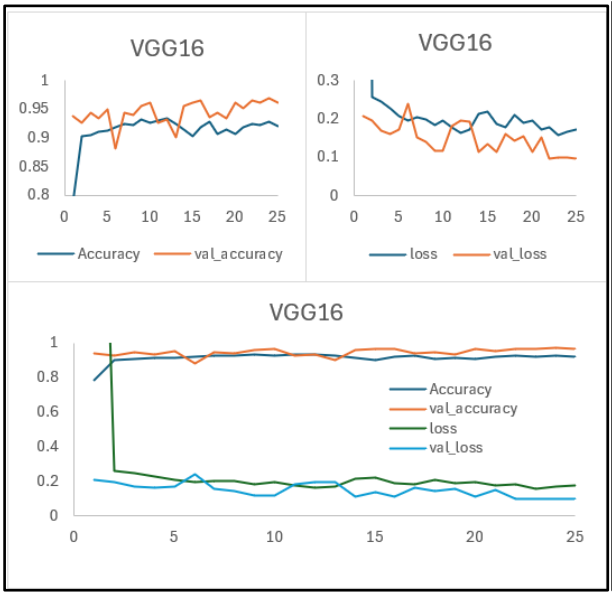

(a) Custom VGG16 Performance Curves

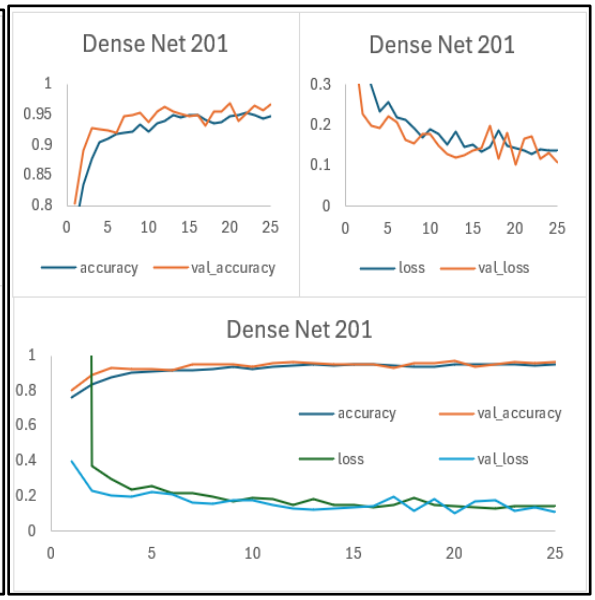

(b) Custom DenseNet 201 Performance Curves

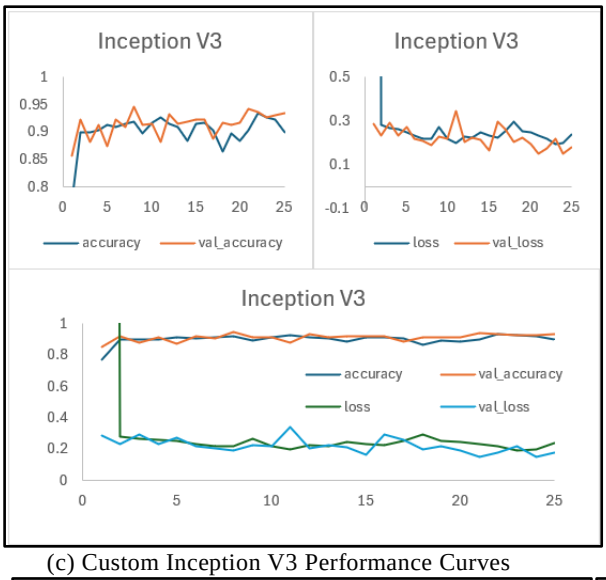

(c) Custom Inception V3 Performance Curves

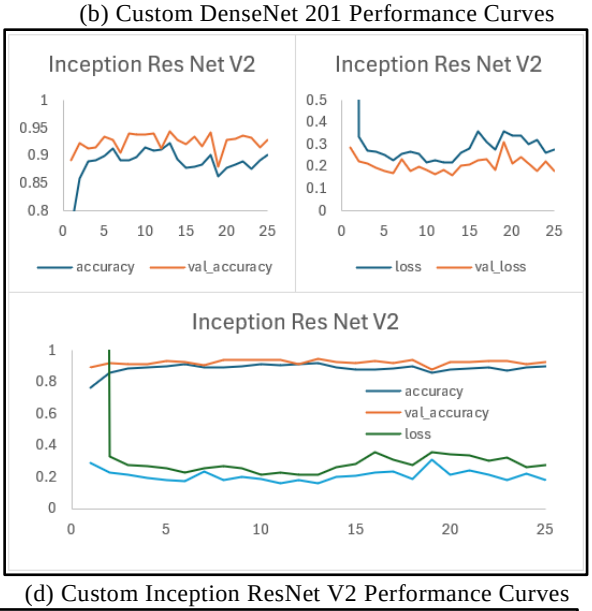

(d) Custom Inception ResNet V2 Performance Curves

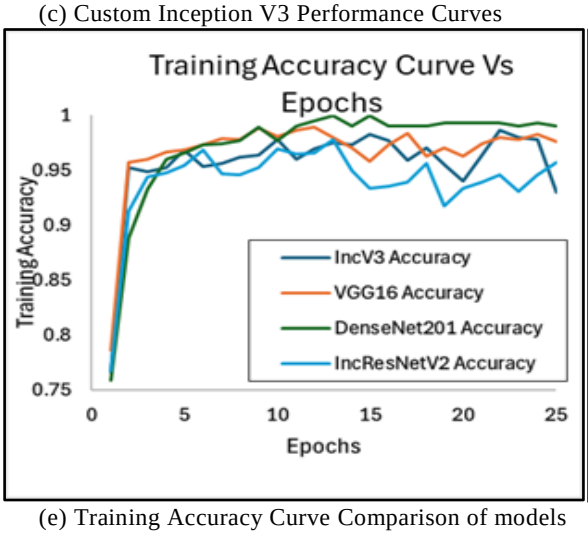

(e) Training Accuracy Curve Comparison of models

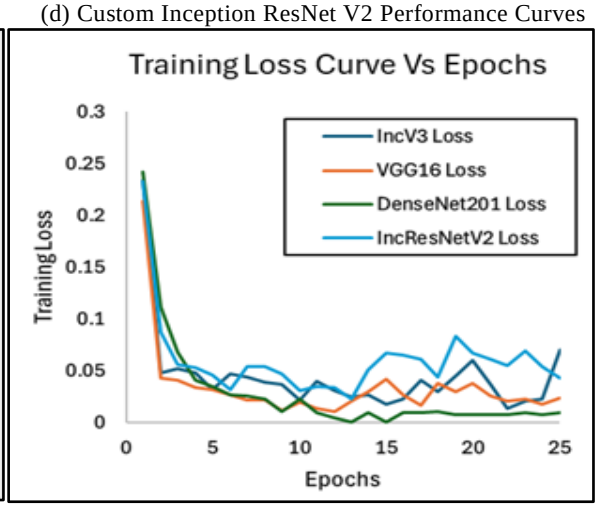

(f) Training Loss Curve Comparison of models

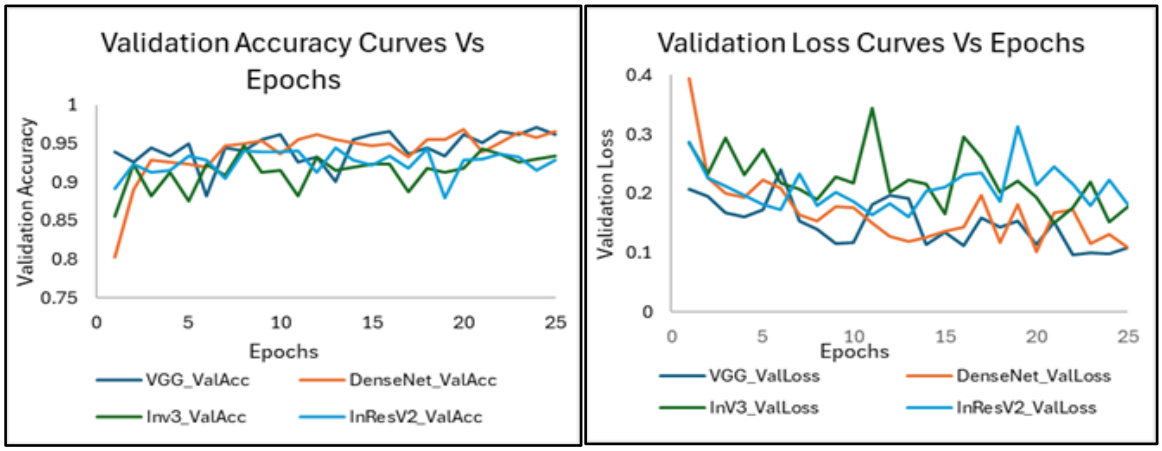

(g) Validation Accuracy Curve Comparison of models (h) Validation Loss Curve Comparison of models

Fig. 16: (a) VGG16 Accuracy & Loss curves (b) Dense Net 201 Accuracy and Loss curves (c) Inception V3 Accuracy and Loss curves (d) Inception Res Net V2 Training accuracy and loss curves (e) Training Accuracy Curves of models (f) Comparison of Training Losses of Models (g) Comparison of Validation Accuracy Curves (h) Comparison of Validation Loss Curves

Fig. 16(e) illuminates the summary of all the deep learning architectures of this study in terms of their training accuracies attained, and Fig. 16(f) illuminates the summary of the loss incurred during the learning process of the training phase. Fig. 16(g) shows the comparison of the validation accuracies of the models, whereas Fig. 16(h) depicts the validation loss comparison of the models. It is visibly evident that the architectures are gradually learning over the course of epochs, as a result, minimizing the loss metric, thus making the deep learning architectures a powerful tool for the implementation and experimentation of the digital complex images.

The inference time is considered a critical metric in the practical deployment of the model. The training per epoch revealed a clear difference in the computational efficiency, with the custom Dense Net 201 demonstrating highly consistent and efficient execution time of 220 222 seconds per epoch. Custom VGG16 model exhibited moderate efficiency in terms of execution time per epoch, which is faster than custom Inception ResNet V2 but slower than the custom Inception V3 in the range of 210 240 seconds. In contrast, Inception V3 is most computationally efficient with relatively less execution time of 186 195 seconds per epoch. However, this comes with the cost of lower accuracy. Meanwhile, custom Inception Res Net V2 demonstrated the poorest and most volatile computational potential, with execution time per epoch taking over 300 seconds, confirming it as the slowest and least computationally efficient model.

The main part of the implementation refers to the evaluation of these deep learning architectures on the unseen unknown samples of the dataset comprising 1217 images of both categories included in the test data. A confusion matrix is the best evaluation tool that is employed to summarize the performance of a model in terms of the true values and predictions made. The accuracy of the model is computed by considering the actual values and the likelihood of predictions. The confusion matrix of the deep learning architectures utilized in this study is given in Fig. 17. In clockwise direction, Fig. 17(a) represents the confusion matrix of the custom VGG model, followed by Fig. 17(b) depicting the metrics of true and false predictions obtained by the custom DenseNet 201 model. The second row - first column has Fig. 17(c) showing the metrics of the custom Inception V3 model, and finally, in Fig. 17(d), the custom Inception Res Net v2 model's performance on the test data is shown as a confusion matrix report. From Figure 18, we can conclude that the performance of models during the testing phase in descending order of accuracy is Dense Net 201(96.3%), Inception Res Net V2(95.6%), VGG16(94.7%), and Inception V3 (93.9%). The accuracy of the models is calculated as the division of the sum of the top-left value and the bottom-right value by the total values in the block. The loss of Dense Net 201 model is comparatively less when compared to VGG16, Inception v3 model, and Inception Res Net v2 models.

Fig. 18(a) depicts the correct predictions of VGG16, DenseNet 201, Inception v3, and Inception Res Net v2 models for the binary classification of chest x-ray. Dense Net 201 has considerably high predictions followed by Inception Res Net v2, VGG16, and Inception v3 models. Fig. 18(b) depicts the incorrect predictions of VGG16, DenseNet 201, Inception v3, and Inception Res Net v2 models for the binary classification of chest x-ray. The predictions that mismatch with the actual label of the image are shown. Inception v3 has more incorrect predictions compared to VGG16, Inception Res Net v2, and Dense Net 201 models.

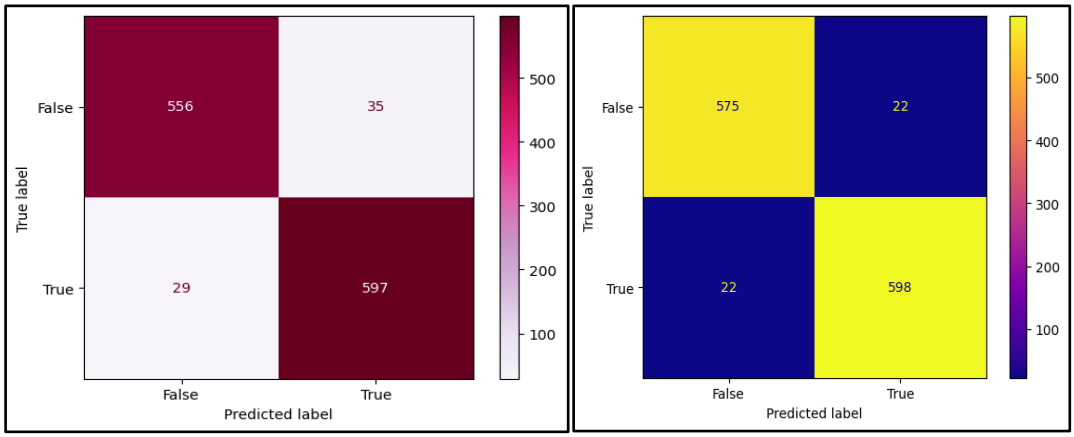

(a) Confusion Matrix of Custom VGG16 (b) Confusion Matrix of Custom DenseNet 201

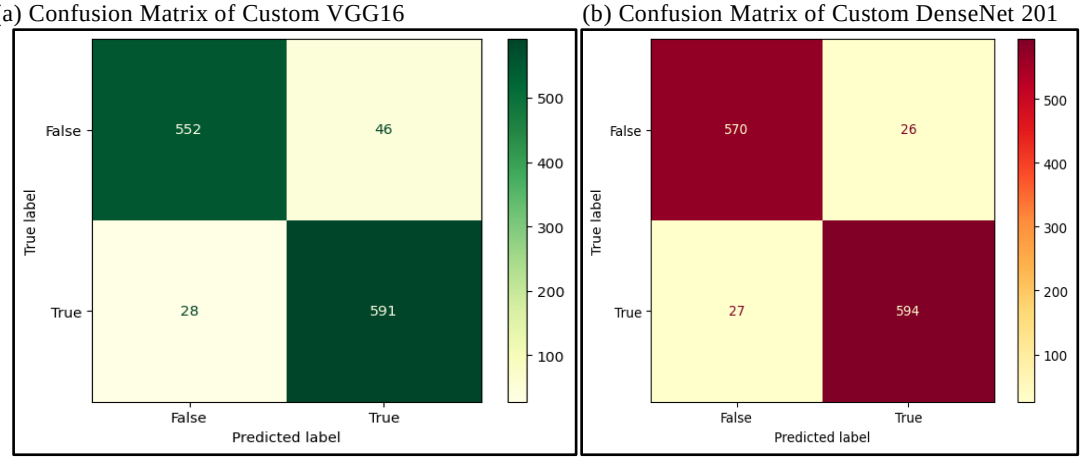

(c) Confusion Matrix of Custom InceptionV3 (d) Confusion Matrix of Custom Inception ResNet V2

Fig. 17: Confusion Matrix of transfer learning-based models

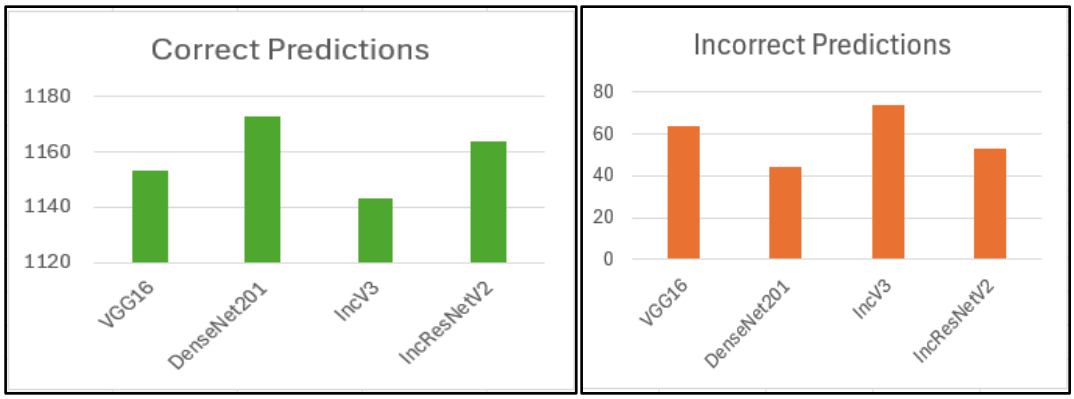

(a) Correct Predictions (b) Incorrect Predictions

Fig. 18: Predictions Summary of models on test data

The performance of each model is linked to its internal design. Dense Net 201 has showcased superior performance because of its dense connections. As layers have direct connections leading to short paths for information to travel, the vanishing gradient problem is reduced, and feature reuse is encouraged, thereby making the model highly effective in spotting the fine, cloudy patterns of pneumonia even with a relatively moderate number of parameters. Inception V3, though a powerful architecture, has shown a lower accuracy as

it is designed to look at the input image at different scales using different filter sizes, thereby making the architecture complex and computationally heavy even in simple, relatively low-complexity classification tasks. VGG16 is a very simple and deep architecture with repeated convolutional layers, but it is computationally expensive and lacks a sophisticated feature propagation mechanism, which restricts its ability to build on features effectively. Inception ResNet V2 has made a strong showing as it combines multi-scale processing from the Inception family and the stability of residual networks in training. The hybrid design has enabled us to learn rich, complex features at different scales, making it one of the effective models, though computationally heavy.

Challenges and Future Research Scope

The main challenges of this study are the availability and gathering of balanced data and scalability, the performance getting affected due to image quality, high-performance hardware, and computation resources like GPU and TPU, and hyper-parameter tuning, as it is time-consuming and computationally intensive. The deployment of AI in healthcare needs to address a few ethical considerations. The models developed are intended as a diagnostic aid and are not a replacement for a qualified professional, and the final responsibility and accountability remain with the human expert. Considering the black box nature of the deep learning architectures, the use of explainable AI techniques needs to be encouraged to gain trust in the model output reasoning for radiologists, enhancing the transparency and explainability aspects of AI systems.

Future research scope is to address the scalability of our model by enriching the training data with variety of imaging environment and observations as large datasets have inter-class similarities and intra-class variations which poses as a concern for model’s performance, to enhance the model’s classification between different types of pneumonia caused by bacteria, virus or fungus each with its own distinctive radiographic features and clinical characteristics, to aid the wide scope of classification of image applications beyond pneumonia detection in chest x-rays where fine-grained pattern recognition is essential like kidney stone problem, satellite image analysis, forest monitoring, wildlife monitoring etc. A prospective multi-center clinical trial for validating the model's ability in real-world settings and shifting focus to assess the clinical impact by measuring radiologist interpretation time, error in diagnosis, which led to the practical testing that can be carried out as an enhancement in the future.

Conclusion

Since the emergence of deep learning, CNNs have progressed continuously with many breakthroughs and innovations, as they contribute to image recognition and classification labels without any reasoning, raising concerns about radiologists' trustworthiness. In the present digital era, the models act as an Assistant (not a replacement) to the radiologist, a future enhancement in diagnostic pathways to assist a clinician who is not an expert in chest x-ray interpretation. The most important requirement for accurate diagnosis of pneumonia is the availability of specialist radiologists. The objective of this study is to enhance medical competence in places where there is limited availability of specialist radiologists and to facilitate the prevention of mortality by early diagnosis of pneumonia. Developing algorithms and models in this domain is highly valuable in healthcare services. Different models, VGG16, DenseNet 201, Inception v3, and Inception Res Net v2, are fine-tuned and used for the evaluation of chest x-ray images to detect the infection. The X-ray images are budget-friendly and have good accessibility. VGG16 model's simple architecture, Dense Net 201's information flow, and the complex pattern recognition of the versions of the Inception model have facilitated the intricate feature extraction, which is crucial in differentiating between normal and pneumonia images. The evaluation of the models VGG16, DenseNet 201, Inception v3, and Inception Res Net v2 is done based on the test accuracy values achieved 94.7%, 96.3%, 93.9% 95.6% respectively. The Dense Net 201 model has achieved comparatively higher results than other models. Comparison of different models of related published work is shown in Table 2.

In conclusion, the VGG16, DenseNet201, InceptionV3, and Inception Res Net v2, through transfer learning, coupled with fine-tuning of their parameters, have proven influential in advancing the domain of pneumonia classification. The combination of transfer learning and parameter fine-tuning has showcased not only the adaptability of these architectures to dedicated medical imaging tasks but also for further precise and efficient diagnosis, eventually benefiting patient care and treatment planning in the realm of pulmonology and infectious diseases.

Standard Notations and Abbreviations

VGG16 Visual Geometry Group with 16 layers.

DENSE NET 201 Dense Convolution Network that is 201 layers deep.

INCEPTION V3 Third version of Inception Convolution Neural Network.

INCEPTION RES NET V2 Second version of Inception Residual Neural Network.

Table 2: Comparison with other researchers' published work

S. No	Method	Testing Accuracy	No of images	Limitation	Reference
1.	AlexNet, ResNet18, Inc v3, Dense Net121, GoogLeNet Ensemble Model	92.8% 94.23% 92.01% 92.62% 93.12% 96.3%	5232 (1346 Normal + 3883 Diseased)	Data imbalance in categories	(Chouhan et al., 2020)
2.	Efficient Net B0 + Dense Net 121 with Multi-Head Attention mechanism	95.19%	5856 (1591 Normal + 4265 Diseased)	Data imbalance in categories	(An et al., 2024)
3.	NN + VGG16	92.16% 95.4%	Dataset1 5856 (1591 Normal + 4265 Diseased) Dataset2 6432 (1583 Normal + 4273 Pneumonia + 576 Covid-19)	Data imbalance in categories	(Jiang et al., 2021)
4.	IVGG13 (Improved VGG16 – reduced VGG16 network depth)	89%	10000 (5000 Normal + 5000 Pneumonia)	Can be enhanced to improve accuracy	(Ni et al., 2024)
5.	VGG16 Dense Net 201 Inception v3 Inception Res Net v2	94.7%, 96.3%, 93.9% 95.6%	6084 (3019 Normal + 3065 Pneumonia)	Scalability - Increase dataset size to ensure a high recognition rate	Proposed work

Acknowledgment

The authors would like to thank the anonymous reviewers for their valuable contributions through suggestions and time in reviewing the research article.

Funding Information

The authors have not received any funding or financial support to report.

Authors Contributions

Nusrath Fathima: contributed to writing and implementation of the manuscript.

Pradeep Kumar: Supervised the research and contributed to structuring the manuscript.

Ethics

This article is original and contains unpublished material. The corresponding author confirms that all of the other authors have read and approved the manuscript, and no ethical issues are involved.

References

Al Mamlook, R. E., Chen, S., & Bzizi, H. F. (2020). *Investigation of the performance of Machine Learning Classifiers for Pneumonia Detection in Chest X-ray Images*. 2020 IEEE International Conference on Electro Information Technology (EIT), Chicago, Illinois, USA. https://doi.org/10.1109/eit48999.2020.9208232

Al-kuraishy, H., Al-Maiahy, T., Al-Gareeb, A., Musa, R., & Ali, Z. (2020). COVID-19 pneumonia in an Iraqi pregnant woman with preterm delivery. *Asian Pacific Journal of Reproduction*, *9*(3), 156–158. https://doi.org/10.4103/2305-0500.282984

An, Q., Chen, W., & Shao, W. (2024). A Deep Convolutional Neural Network for Pneumonia Detection in X-ray Images with Attention Ensemble. *Diagnostics*, *14*(4), 390. https://doi.org/10.3390/diagnostics14040390

Asif, S., Wenhui, Y., Amjad, K., Jin, H., Tao, Y., & Jinhai, S. (2023). Detection of COVID-19 from chest X-ray images: Boosting the performance with convolutional neural network and transfer learning. *Expert Systems*, *40*(1), e13099. https://doi.org/10.1111/exsy.13099

Attallah, O. (2021). MB-AI-His: Histopathological Diagnosis of Pediatric Medulloblastoma and its Subtypes via AI. *Diagnostics*, *11*(2), 359. https://doi.org/10.3390/diagnostics11020359

Asswin, C. R., KS, D. K., Dora, A., Ravi, V., Sowmya, V., Gopalakrishnan, E. A., & Soman, K. P. (2023). Transfer learning approach for pediatric pneumonia diagnosis using channel attention deep CNN architectures. *Engineering Applications of Artificial Intelligence*, *123*, 106416. https://doi.org/10.1016/j.engappai.2023.106416

Baltruschat, I. M., Nickisch, H., Grass, M., Knopp, T., & Saalbach, A. (2019). Comparison of Deep Learning Approaches for Multi-Label Chest X-Ray Classification. In *Scientific Reports* (Vol. 9, Issue 1, p. 6381). https://doi.org/10.1038/s41598-019-42294-8

Berliner, D., Schneider, N., Welte, T., & Bauersachs, J. (2 016). The Differential Diagnosis of Dyspnea. In *Deutsches Ärzteblatt international* (Vol. 113, Issue 49, pp. 834–845). https://doi.org/10.3238/arztebl.2016.0834

Bhattarai, P & Od, R. (2023). *Detection of Pneumonia using Machine Learning* (pp. 1–11). https://doi.org/10.1145/3647444.3652464

Boesch, G. (2021). *Very deep convolutional networks (vgg) essential guide*.

Brital, A. (2021). Inception V4 Convolutional Neural Network (CNN) For Accuracy Improvement. In *Revista Gestão Inovação e Tecnologias* (Vol. 11, Issue 4, pp. 1138–1148). https://doi.org/10.47059/revistageintec.v11i4.2174

Chakraborty, S., Nag, T., Pandey, S. K., Ghosh, J., & Dey, L. (2025). Deep Learning and X-Ray Imaging Innovations for Pneumonia Infection Diagnosis: Introducing DeepPneuNet. In *Computational Intelligence* (Vol. 41, Issue 1, p. e70029). https://doi.org/10.1111/coin.70029

Chhabra, M., & Kumar, R. (2022). *An Advanced VGG16 Architecture-Based Deep Learning Model to Detect Pneumonia from Medical Images* (pp. 457–471). Springer. https://doi.org/10.1007/978-981-16-8774-7_37

Chouhan, V., Singh, S. K., Khamparia, A., Gupta, D., Tiwari, P., Moreira, C., Damaševičius, R., & de Albuquerque, V. H. C. (2020). A Novel Transfer Learning Based Approach for Pneumonia Detection in Chest X-ray Images. In *Applied Sciences* (Vol. 10, Issue 2, p. 559). https://doi.org/10.3390/app10020559

Colin, J., & Surantha, N. (2025). Interpretable Deep Learning for Pneumonia Detection Using Chest X-Ray Images. In *Information* (Vol. 16, Issue 1, p. 53). https://doi.org/10.3390/info16010053

El Asnaoui, K., Chawki, Y., & Idri, A. (2021). Automated Methods for Detection and Classification Pneumonia Based on X-Ray Images Using Deep Learning. *Health Informatics: A Computational Perspective in Healthcare*, *90*, 257–284. https://doi.org/10.1007/978-3-030-74575-2_14

Elgendy, M. (2020). *Deep Learning for Vision Systems*.

Elgendy, M., Balaha, H. M., Shehata, M., Alksas, A., Ghoneim, M., Sherif, F., Mahmoud, A., Elgarayhi, A., Taher, F., Sallah, M., Ghazal, M., & El-Baz, A. (2022). Role of Imaging and AI in the Evaluation of COVID-19 Infection: A Comprehensive Survey. *Frontiers in Bioscience-Landmark*, *27*(9). https://doi.org/10.31083/j.fbl2709276

El-Latif, E. I. A., El-dosuky, M., Darwish, A., & Hassanien, A. E. (2024). A deep learning approach for ovarian cancer detection and classification based on fuzzy deep learning. *Scientific Reports*, *14*(1), 26463. https://doi.org/10.1038/s41598-024-75830-2

Gabruseva, T., Poplavskiy, D., & Kalinin, A. (2020). *Deep Learning for Automatic Pneumonia Detection*. 2020 IEEE/CVF Conference on Computer Vision and Pattern Recognition Workshops (CVPRW), Seattle, WA, USA. https://doi.org/10.1109/cvprw50498.2020.00183

Gupta, H., Bansal, N., Garg, S., Mallik, H., Prabha, A., & Yadav, J. (2023). A hybrid convolutional neural network model to detect COVID-19 and pneumonia using chest X-ray images. *International Journal of Imaging Systems and Technology*, *33*(1), 39–52. https://doi.org/10.1002/ima.22829

Hammoudi, K., Benhabiles, H., Melkemi, M., Dornaika, F., Arganda-Carreras, I., Collard, D., & Scherpereel, A. (2021). Deep Learning on Chest X-ray Images to Detect and Evaluate Pneumonia Cases at the Era of COVID-19. *Journal of Medical Systems*, *45*(7), 75. https://doi.org/10.1007/s10916-021-01745-4

Hesamian, M. H., Jia, W., He, X., & Kennedy, P. (2019). Deep Learning Techniques for Medical Image Segmentation: Achievements and Challenges. *Journal of Digital Imaging*, *32*(4), 582–596. https://doi.org/10.1007/s10278-019-00227-x

Ibrahim, A. U., Ozsoz, M., Serte, S., Al-Turjman, F., & Yakoi, P. S. (2024). Pneumonia Classification Using Deep Learning from Chest X-ray Images During COVID-19. *Cognitive Computation*, *16*(4), 1589–1601. https://doi.org/10.1007/s12559-020-09787-5

Jain, D. K., Singh, T., Saurabh, P., Bisen, D., Sahu, N., Mishra, J., & Rahman, H. (2022). Deep Learning-Aided Automated Pneumonia Detection and Classification Using CXR Scans. *Computational Intelligence and Neuroscience*, *2022*(1), 7474304. https://doi.org/10.1155/2022/7474304

Jain, R., Singh, P., & Kaur, A. (2024). An ensemble reinforcement learning-assisted deep learning framework for enhanced lung cancer diagnosis. *Swarm and Evolutionary Computation*, *91*, 101767. https://doi.org/10.1016/j.swevo.2024.101767

Jaiswal, A., Gianchandani, N., Singh, D., Kumar, V., & Kaur, M. (2021). Classification of the COVID-19 infected patients using DenseNet201 based deep transfer learning. *Journal of Biomolecular Structure and Dynamics*, *39*(15), 5682–5689. https://doi.org/10.1080/07391102.2020.1788642

Jeong, H., Kim, H., Yoon, J., Go, K., & Gwak, J. (2022). OVASO: Integrated binary CNN models to classify COVID>-19, pneumonia and healthy lung in X-ray images. *International Journal of Imaging Systems and Technology*, *32*(4), 1035–1048. https://doi.org/10.1002/ima.22742

Jiang, Z.-P., Liu, Y.-Y., Shao, Z.-E., & Huang, K.-W. (2021). An Improved VGG16 Model for Pneumonia Image Classification. *Applied Sciences*, *11*(23), 11185. https://doi.org/10.3390/app112311185

Johnson, S., & Wells, D. (2019). Healthline Viral Pneumonia: Symptoms, Risk Factors, and More. *Healthline*.

Lamia, A., & Fawaz, A. (2022). Detection of Pneumonia Infection by Using Deep Learning on a Mobile Platform. *Computational Intelligence and Neuroscience*, *2022*(1), 7925668. https://doi.org/10.1155/2022/7925668

Le Cun, Y., Bengio, Y., & Hinton, G. (2015). Deep learning. *Nature*, *521*(7553), 436–444. https://doi.org/10.1038/nature14539

Liang, G., & Zheng, L. (2020). A transfer learning method with deep residual network for pediatric pneumonia diagnosis. *Computer Methods and Programs in Biomedicine*, *187*, 104964. https://doi.org/10.1016/j.cmpb.2019.06.023

Mahum, R., Munir, H., Mughal, Z.-U.-N., Awais, M., Sher Khan, F., Saqlain, M., Mahamad, S., & Tlili, I. (2023). A Novel Framework for Potato leaf Disease Detection using an Efficient Deep Learning Model. In *Human and Ecological Risk Assessment: An International Journal* (Vol. 29, Issue 2, pp. 303–326). https://doi.org/10.1080/10807039.2022.2064814

Mathivanan, S. K., Sonaimuthu, S., Murugesan, S., Rajadurai, H., Shivahare, B. D., & Shah, M. A. (2024). Employing deep learning and transfer learning for accurate brain tumor detection. *Scientific Reports*, *14*(1). https://doi.org/10.1038/s41598-024-57970-7

Mavaddati, S. (2024). Brain tumors classification using deep models and transfer learning. *Multimedia Tools and Applications*, *84*(22), 25677–25708. https://doi.org/10.1007/s11042-024-20141-x

Mohamed Abueed, M. A., Nor, D. M., Ibrahim, N., & Ogier, J.-M. (2025). Pneumonia Detection Using Transfer Learning: A Systematic Literature Review. *International Journal of Advanced Computer Science and Applications*, *16*(2). https://doi.org/10.14569/ijacsa.2025.01602102

Motamed, S., Rogalla, P., & Khalvati, F. (2021). Data augmentation using Generative Adversarial Networks (GANs) for GAN-based detection of Pneumonia and COVID-19 in chest X-ray images. *Informatics in Medicine Unlocked*, *27*, 100779. https://doi.org/10.1016/j.imu.2021.100779

Nguyen, L. D., Lin, D., Lin, Z., & Cao, J. (2018). *Deep CNNs for microscopic image classification by exploiting transfer learning and feature concatenation*. 1–5. https://doi.org/10.1109/iscas.2018.8351550

Ni, Y., Cong, Y., Zhao, C., Yu, J., Wang, Y., Zhou, G., & Shen, M. (2024). Active learning based on multi-enhanced views for classification of multiple patterns in lung ultrasound images. *Computerized Medical Imaging and Graphics*, *118*, 102454. https://doi.org/10.1016/j.compmedimag.2024.102454

Ouis, M. Y., & A. Akhloufi, M. (2024). Deep learning for report generation on chest X-ray images. *Computerized Medical Imaging and Graphics*, *111*, 102320. https://doi.org/10.1016/j.compmedimag.2023.102320

Pan, S. J., & Yang, Q. (2010). A Survey on Transfer Learning. *IEEE Transactions on Knowledge and Data Engineering*, *22*(10), 1345–1359. https://doi.org/10.1109/tkde.2009.191

Patil, N., Doshi, A., & Dodiya, V. (2024). *Pneumonia Detection Using Deep Neural Networks Based on Chest X-ray Images*. 395–406. https://doi.org/10.1007/978-981-97-0327-2_29

Phine, S. (2023). *Pneumonia Classification Using Deep Learning VGG19 Model*. 67–71. https://doi.org/10.1109/icca51723.2023.10181954

Rahman, T., Chowdhury, M. E. H., Khandakar, A., Islam, K. R., Islam, K. F., Mahbub, Z. B., Kadir, M. A., & Kashem, S. (2020). Transfer Learning with Deep Convolutional Neural Network (CNN) for Pneumonia Detection Using Chest X-ray. *Applied Sciences*, *10*(9), 3233. https://doi.org/10.3390/app10093233

Sait, U., Shivakumar, S., K V, G. L., Kumar, T., Ravishankar, V. D., & Bhalla, K. (2019). *A Mobile Application for Early Diagnosis of Pneumonia in the Rural context*. 1–5. https://doi.org/10.1109/ghtc46095.2019.9033048

Sanghvi, H. A., Patel, R. H., Agarwal, A., Gupta, S., Sawhney, V., & Pandya, A. S. (2023). A deep learning approach for classification of COVID and pneumonia using DenseNet-201. *International Journal of Imaging Systems and Technology*, *33*(1), 18–38.https://doi.org/10.1002/ima.22812

Sarvari, A. V. P., & Sridevi, K. (2025). Optimized Residual Attention Based Generalized Adversarial Network for COVID-19 Classification Using Chest CT Images. *Computational Intelligence*, *41*(2), e70031. https://doi.org/10.1111/coin.70031

Sevli, O. (2022). A deep learning-based approach for diagnosing COVID-19 on chest x-ray images, and a test study with clinical experts. *Computational Intelligence*, *38*(5), 1659–1683. https://doi.org/10.1111/coin.12526

Sharma, S., & Guleria, K. (2023). A Deep Learning based model for the Detection of Pneumonia from Chest X-Ray Images using VGG-16 and Neural Networks. *Procedia Computer Science*, *218*, 357–366. https://doi.org/10.1016/j.procs.2023.01.018

Shin, H.-C., Roth, H. R., Gao, M., Lu, L., Xu, Z., Nogues, I., Yao, J., Mollura, D., & Summers, R. M. (2016). Deep Convolutional Neural Networks for Computer-Aided Detection: CNN Architectures, Dataset Characteristics and Transfer Learning. *IEEE Transactions on Medical Imaging*, *35*(5), 1285–1298. https://doi.org/10.1109/tmi.2016.2528162

Siddiqi, R., & Javaid, S. (2024). Deep Learning for Pneumonia Detection in Chest X-ray Images: A Comprehensive Survey. *Journal of Imaging*, *10*(8), 176. https://doi.org/10.3390/jimaging10080176

Sirish Kaushik, V., Nayyar, A., Kataria, G., & Jain, R. (2020). Pneumonia Detection Using Convolutional Neural Networks (CNNs). *Proceedings of First International Conference on Computing, Communications, and Cyber-Security (IC4S 2019)*, *121*, 471–483. https://doi.org/10.1007/978-981-15-3369-3_36

Sitaula, C., & Hossain, M. B. (2021). Attention-based VGG-16 model for COVID-19 chest X-ray image classification. In *Applied Intelligence* (Vol. 51, Issue 5, pp. 2850–2863). https://doi.org/10.1007/s10489-020-02055-x

Srivastav, D., Bajpai, A., & Srivastava, P. (2021). Improved Classification for Pneumonia Detection using Transfer Learning with GAN based Synthetic Image Augmentation. *Proceedings of the 2021 11th International Conference on Cloud Computing, Data Science & Engineering (Confluence)*, 967–972. https://doi.org/10.1109/confluence51648.2021.9377062

Stephen, O., Sain, M., Maduh, U. J., & Jeong, D.-U. (2019). An Efficient Deep Learning Approach to Pneumonia Classification in Healthcare. *Journal of Healthcare Engineering*, *2019*(1), 4180949. https://doi.org/10.1155/2019/4180949

Shu, M. (2019). *Deep learning for image classification on very small datasets using transfer learning*. https://doi.org/10.31274/cc-20240624-493

Swetha, K. R., M, N., P, A. M., & M, M. Y. (2021). *Prediction of Pneumonia Using Big Data, Deep Learning and Machine Learning Techniques*. 1066–1071. https://doi.org/10.1109/icces51350.2021.9489188

Szepesi, P., & Szilágyi, L. (2022). Detection of pneumonia using convolutional neural networks and deep learning. *Biocybernetics and Biomedical Engineering*, *42*(3), 1012–1022. https://doi.org/10.1016/j.bbe.2022.08.001

Trivedi, M., & Gupta, A. (2022). A lightweight deep learning architecture for the automatic detection of pneumonia using chest X-ray images. *Multimedia Tools and Applications*, *81*(4), 5515–5536. https://doi.org/10.1007/s11042-021-11807-x

University of Utah Health. (2024). *404 - Page Not Found*. https://healthcare.utah.edu/pulmonary/conditions/pneumonia.

Wager, S., Wang, S., & Liang, P. (2013). Dropout Training as Adaptive Regularization. *ArXiv*, 1–14.

Xu, W., Chen, B., Shi, H., Tian, H., & Xu, X. (2022). Real-time COVID-19 detection over chest x-ray images in edge computing. *Computational Intelligence*, *39*(1), 36–57. https://doi.org/10.1111/coin.12528